Macromolecules

Cite This: Macromolecules 2019, 52, 620−628

Article

pubs.acs.org/Macromolecules

Charge Transport in Imidazolium-Based Homo- and Triblock Poly(ionic liquid)s

Emmanuel U. Mapesa,[†] Mingtao Chen,[‡] Maximilian F. Heres,[†] Matthew A. Harris,[†] Thomas Kinsey,[†] Yangyang Wang,[§] Timothy E. Long,[‡] Bradley S. Lokitz,*[,§] and Joshua R. Sangoro*[,†]

[†]Department of Chemical and Biomolecular Engineering, University of Tennessee, Knoxville, 1512 Middle Drive, Knoxville, Tennessee 37996, United States

[‡]Department of Chemistry, Macromolecules Innovation Institute (MII), Virginia Tech, Blacksburg, Virginia 24061, United States

[§]Center for Nanophase Materials Sciences, Oak Ridge National Laboratory, One Bethel Valley Road, Oak Ridge, Tennessee 37830, United States

Supporting Information

ABSTRACT: Ion dynamics in a series of imidazolium-based triblock copolymers (triblock co-PILs) are investigated using broadband dielectric spectroscopy (BDS) and differential scanning calorimetry (DSC) and compared to their homopolymer counterparts (homo-PILs). Two calorimetric glass transition temperatures (T_g) are observed corresponding to the charged poly(ionic liquid) (PIL) blocks and noncharged polystyrene (PS) blocks. Varying the counterion from Br^- to NTf_2^- decreases the T_g of the charged block by over 50 °C, thereby increasing the room-temperature ionic dc conductivity by over 6 orders of magnitude. Interestingly, for a given anion, varying the volume fraction of the charged block, from ∼0.5 to ∼0.8, has very minimal effect on the dc ionic conductivity, indicating that the choice of counterion is the key factor influencing charge transport in these systems.

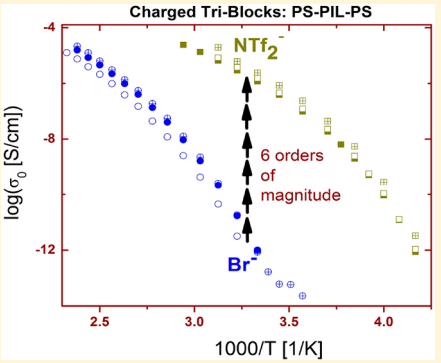

INTRODUCTION

Ionic liquids (ILs)—molten salts with melting temperature below 100 °C—continue to receive concerted research interest because of their potential for applications in energy storage and electrochemical devices.[1−3] Besides their high ionic conductivity (in the mS/cm range), the negligible vapor pressure and high thermal and electrochemical stability of ILs present significant advantages over conventional solvent-based electrolytes and make them candidates for applications in solid electrolytes,[2,4−8] ion exchange membranes (IEMs),[9,10] actuators,[11−13] and gas separation membranes.[14−16] Because liquid electrolytes have the intrinsic problem of leakage, polymerized ionic liquids offer a better route for utilizing ILs since, ideally, they combine desirable mechanical properties of polymers with the high conductivity of ILs.[17,18]

Homo-poly(ionic liquid)s or segmented copolymers have demonstrated tunable mechanical properties with reasonable ionic conductivity in the semiconductor range at temperatures above the glass transition temperature (T_g). For instance, Hemp et al. synthesized ammonium- and phosphonium-based homo-PILs with T_g ranging from 62 to 91 °C.[19] At 100 °C, they exhibited ionic conductivities in the range 10^{-7}−10^{-5} S/cm. Wang et al. studied segmented polyurethanes and reported tunable T_gs depending on counterion identities; the systems demonstrated appreciable ionic conductivities (∼10^{-6} S/cm) at 50 K above T_g.[20] On the other hand, Jourdain et al. achieved high ionic conductivity (7×10^{-5} S/cm) at room temperature using siloxane-based homo-PILs at the cost of mechanical properties (T_g = −62 °C).[21] Evidently, in the cases of homopolymers and segmented copolymers, ion dynamics and structural relaxation are strongly correlated above T_g, leading to an ostensibly inevitable, and significant, trade-off between ionic conductivity and mechanical integrity.[20−23]

It has been demonstrated that ion conduction in homo-PILs can be decoupled from structural relaxation.[24,25] This phenomenon has therefore been suggested as a plausible route to obtaining homo-PILs with desirable properties. Fan et al. probed the effect of changing pendant groups and found that adding shorter flexible tails to the charged side group enhances decoupling of ionic conductivity,[26] much in agreement with similar studies.[27,28] Other factors that have been shown to influence decoupling include molecular weight[29] and application of pressure.[30] Put together, these studies suggest that frustration in chain packing of the polymeric cation, and hence free volume, plays a key role in determining the degree of decoupling of ion conductivity from structural dynamics. Nevertheless, up to now, desirable levels of ion conductivity for applications have not been achieved via enhancement of the extent decoupling of ion conductivity.

Received: October 5, 2018
Revised: December 14, 2018
Published: January 3, 2019

DOI: 10.1021/acs.macromol.8b02143
Macromolecules 2019, 52, 620−628

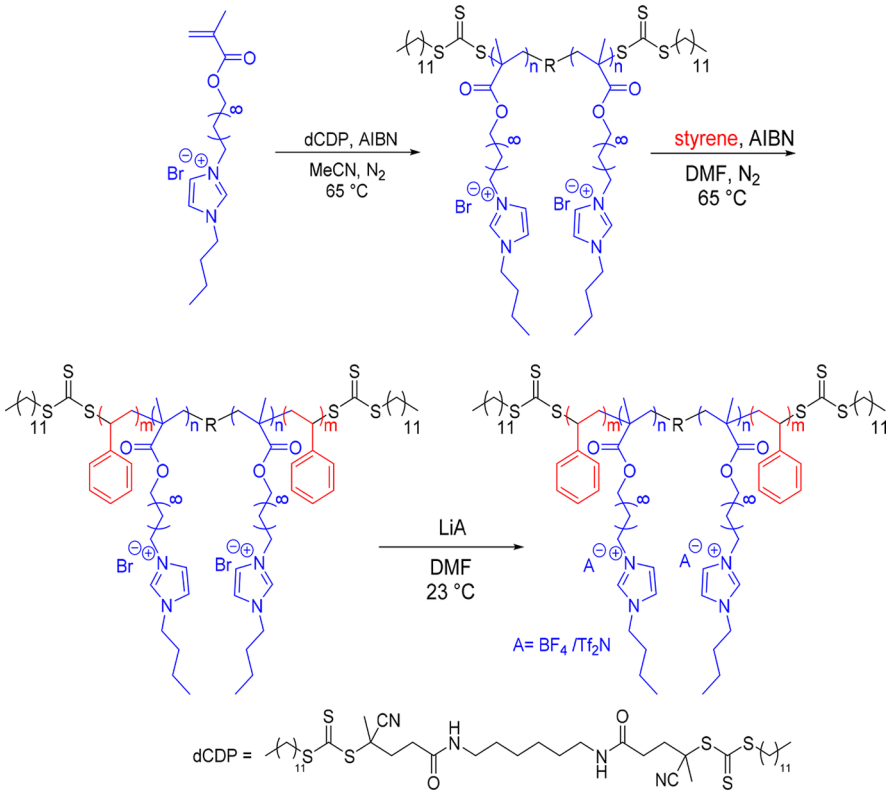

Figure 1. Two-step, divergent synthesis of poly(1BDIMABr) macroCTA and poly(S-*b*-1BDIMABr-*b*-S) ABA triblock copolymers using difunctional CTA in RAFT polymerization.

The continued quest for materials that bear both high conductivity and high elastic modulus has therefore led to interest in polymers that undergo microphase separation into hard and soft domains.[2,8,31−41] The soft domains are expected to provide a path for ion transport while the hard ones offer high elastic modulus, effectively enabling the processing of free-standing films. Park and co-workers achieved ionic conductivity as high as 10^{-2} S/cm at 100 °C after introducing favorable microphase morphologies in PS-*b*-PEO diblock copolymers.[8] Recently, some of the coauthors of the current article reported the synthesis of novel homo-PILs composed of methacrylate backbones and imidazolium pendant groups spaced by a long alkyl linkage; the homo-PILs exhibited promising ionic conductivity as high as 2.45×10^{-5} S/cm, although the corresponding T_gs remained below 10 °C.[42] In this work, ABA-type triblock copolymer analogues of the said homo-PILs-containing styrene (S) and the ionic liquid monomers, 1-[ω-methacryloyloxydecyl]-3-(n-butyl)-imidazolium bromide (1BDIMABr), are probed by differential scanning calorimetry (DSC) and broadband dielectric spectroscopy (BDS). We compare ion dynamics in the triblock co-PILs to that of the corresponding homo-PILs and show that the main factor influencing ion dynamics in triblock co-PILs is the type of anion. This work demonstrates that it is possible to improve the mechanical properties of triblock co-PILs without compromising ionic conductivity.

EXPERIMENTAL SECTION

Materials. Lithium tetrafluoroborate (98%), bis(trifluoromethane)sulfonimide lithium salt, 10-bromo-1-decanol (technical grade, 90%), 1-butylimidazole, triethylamine, and all common organic solvents were purchased from Sigma-Aldrich and used as received. The anhydrous solvents *N*,*N*-dimethylformamide (DMF, 99.8%) and acetonitrile (MeCN, ≥99.8%) were purchased from Sigma-Aldrich and used without further purification. 4-Cyano-4-[(dodecylsulfanylthiocarbonyl)sulfanyl]pentanoic acid (CDP, 97%, HPLC) and 2,2′-azobis(2-methylpropionitrile) (AIBN, 98%) from Sigma-Aldrich were stored at −20 °C and recrystallized once from methanol prior to use. Methacryloyl chloride (≥97.0%, GC, contains ∼0.02% 2,6-di-*tert*-butyl-4-methylphenol as stabilizer) was purchased from Sigma-Aldrich and stored under an inert atmosphere at 2 °C. Styrene was purchased from Sigma-Aldrich and passed through an aluminum oxide column to remove the inhibitor before use. The synthesis of the 1BDIMABr monomer and the use of the difunctional chain transfer agent (CTA, dCDP) for synthesis are described elsewhere.[42,43]

Methods. ^{1}H and ^{19}F nuclear magnetic resonance (NMR) spectroscopy measurements were conducted on a Varian Unity 400 MHz NMR spectrometer (deuterated MeCN or DMSO, 128 scans). Thermal degradation under an N_2 environment was determined by a TA Q500 thermogravimetric analyzer (TGA) at 10 °C/min ramp rate (25 to 600 °C). A TA Q2000 differential scanning calorimeter (DSC) was applied to investigate thermal transitions. Reported values (midpoint) were determined from the second cooling cycle of a heat/cool/heat procedure: (1) 10 °C/min ramp from 23 to 150 °C, isotherm at 150 °C for 30 min, (2) 100 °C/min quench cool to −80 °C, and (3) 10 °C/min ramp to 150 °C. The total molecular weight and molecular weight distribution of triblock copolymers were determined through size exclusion chromatography (SEC) in DMF (with 0.05 mol of LiBr) at 60 °C at a flow rate of 1 mL/min. The SEC system consists of a Waters 515 HPLC pump equipped with a Waters 717 plus autosampler. Absolute molecular weight was determined through a Wyatt Technology miniDawn MALLS detector operating at 690 nm and a Waters 2414 refractive index detector operating at 880 nm. Specific refractive index values (dn/dc) were determined via an offline Optilab T-rEX refractometer (λ = 658 nm) and were used to calculate weight-average molecular weight (M_w) from SEC. The molecular weights of individual blocks were determined by comparing the peak integral of aromatic peaks in the styrene repeating units

DOI: 10.1021/acs.macromol.8b02143
Macromolecules 2019, 52, 620−628

Table 1. Molecular Weights and T_gs of Triblock Co-PILs with Different Counterions

M_n (kg/mol)	3−34−3			9−34−9			15−34−15		
PDI	1.55			1.35			1.35		
counterions	Br	BF_4	NTf_2	Br	BF_4	NTf_2	Br	BF_4	NTf_2
T_g1 (±2 °C)	21	−12	−33	22	−9	−35	22	−10	−31
T_g2 (±2 °C)	N[a]	N	N	100	98	91	103	101	101

[a]N: not observed.

(6.5−7.5 ppm) and imidazolium peaks in ionic liquid repeating units (8.1−8.4 ppm) through ^{1}H NMR spectroscopy.

Broadband dielectric spectroscopy (BDS) measurements were conducted on a Novocontrol High-Resolution Dielectric Alpha analyzer. The samples were pressed between cylindrical brass electrodes to a thickness of 100 μm. To ensure consistent sample thickness, two silica spacer rods (100 μm diameter) were inserted into the sample before pressing. To erase their thermal history, the samples were thermally equilibrated at 150 °C in a dry nitrogen atmosphere after pressing and prior to BDS measurements. The temperature was controlled by a Quatro cryostat with an accuracy of ±0.1 °C. Frequency sweeps over the range 0.1 Hz−10 MHz were performed at temperatures between 430 and 230 K in steps of 5 K in a cooling−heating−cooling procedure to check for thermal stability and reproducibility of the samples.

Synthesis. *Synthesis of Poly(1BDIMABr) MacroCTA.* A solution of 1-[ω-methacryloyloxydecyl]-3-(n-butyl)imidazolium bromide (1BDIMABr) monomer (10.5 g, 24.5 mmol), dCDP (0.144 g, 0.16 mmol), and AIBN (13.4 mg, 0.08 mmol) in 24.5 mL of MeCN ([1BDIMABr] = 1 M) was purged with argon for 20 min prior to polymerization. The polymerization was performed at 65 °C for a given time to target specific molecular weights. The resulting polymers were precipitated into ethyl acetate and washed with ethyl acetate twice to yield a brown, glue-like product. The product was further dried under vacuum at 50 °C to yield a brown sticky solid. ^{1}H NMR spectroscopy (DMF-d_7, 400 Hz): 0.8−2.2 ppm (polymer backbone and methylenes in pendant groups), 4.0 ppm (2H, CH_2−O−C═O), 4.5 ppm (4H, CH_2−N═C), 8.2 ppm (2H, CH═CH−N), 10.3 ppm (1H, N−CH═N).

Synthesis and Characterization of Poly(S-b-1BDIMABr-b-S) Triblock Copolymers. Styrene monomer (9.8 g), poly(1BDIMABr) macroCTA (5.9 g), and AIBN (12.9 mg) were dissolved in 47.05 mL of DMF. The CTA/I ratio was set to 3/1, and monomer concentration [M] = 2 M. The reaction solution was purged with argon for 40 min prior to polymerization. The polymerization was conducted at 65 °C and quenched by exposing the reaction to air. The resulting polymers were precipitated into ethyl acetate and washed with ethyl acetate three times before drying under vacuum at 50 °C for 24 h. The final product was a light-brown solid. The ion exchange procedure is described elsewhere.[42] ^{1}H NMR spectroscopy (DMF-d_7, 400 Hz): 0.8−2.2 ppm (polymer backbone and methylene protons in pendant groups), 4.0 ppm (2H, CH_2−O−C═O), 4.5 ppm (4H, CH_2−N═C), 6.5−7.5 ppm (aromatic protons, integral depends on composition), 8.2 ppm (2H, CH═CH−N), 10.3 ppm (1H, N−CH═N).

The synthesis of poly(S-b-1BDIMABr-b-S) triblock copolymers involved a two-step RAFT polymerization procedure using difunctional chain transfer agents (CTAs). As illustrated in Figure 1, AIBN thermally initiated the polymerization of 1BDIMABr monomers and produced poly(1BDIMABr) macroCTA after quench and purification. The poly(1BDIMABr) macroCTA was further chain extended with styrene monomers on both ends, and poly(S-b-1BDIMABr-b-S) triblock copolymers were synthesized with three different styrene contents. The use of difunctional CTA allows minimal reinitiation times which are beneficial for a narrow molecular weight distribution.[44] Postpolymerization ion exchange in DMF produced triblock copolymers with different counteranions but identical polymer backbones. ^{1}H NMR spectroscopy confirmed facile and complete anion exchange as evidenced by the complete shift of imidazolium protons (see Figure S1). Triblock copolymers with bromide (Br), tetrafluoroborate (BF_4), and bis(trifluoromethane)-sulfonimide (NTf_2) anions provided an appreciable variation of the T_gs (of the ionic block).

Increasing polymerization time of the styrene monomers led to lower elution time (higher molecular weight) as well as improvement in signal-to-noise ratios. Poly(1BDIMABr) macroCTA exhibited lower refractive index value (dn/dc) than the mobile phase (DMF + 0.05 M LiBr), and the incorporation of styrene blocks increased the refractive index value, resulting in a better signal-to-noise ratio. The triblock copolymers were not soluble in any other common SEC solvents (i.e., chloroform, THF, and water). The absolute molecular weights of three different triblock copolymers were determined using dn/dc values measured offline, and the relative ratios between two blocks were calculated using ^{1}H NMR spectroscopy. Table 1 summarizes the molecular weights of three triblock copolymers: 3−34−3 kg/mol, 9−34−9 kg/mol, and 15−34−15 kg/mol. The polydispersity index (PDI) of the block copolymers decreased with increasing polymerization time, which is as a common trend in RAFT polymerization. To achieve reasonable conversion during the slow propagation of styrene, a relatively low chain transfer agent/initiator (CTA/I) ratio of 3 was employed, leading to overall higher PDI.

Figure 2 demonstrates the thermal transitions of poly(S-b-1BDIMABr-b-S) for samples with molecular weight of 15−34−15

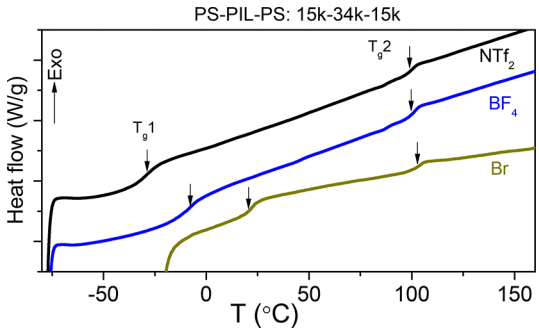

Figure 2. Thermal transitions monitored through DSC thermograms for three samples with the longest uncharged blocks studied (15−34−15 kg/mol). The arrows indicate the respective T_g values.

kg/mol. T_g1 (from −30 to 20 °C) is attributed to the T_g of PIL blocks as the long alkyl spacer linkages between polymer backbones and imidazolium groups offered extra mobility leading to decrease in the T_g. These values are comparable to those reported for the corresponding homo-PILs.[42] T_g2 corresponds well to the T_g (∼100 °C) of polystyrene. Variation of counterions results in no appreciable effect on the T_g of the polystyrene blocks (T_g2). For triblock copolymers with the same counterions but different compositions, minimal changes are observed for both T_g1 and T_g2 (Table 1). In the case of triblock copolymers with 3−34−3 kg/mol molecular weight, the polystyrene blocks were too short to exhibit a prominent T_g, at least as measured by DSC. Overall, the presence of two distinct T_gs in the triblock co-PILs indicates microphase separation. Dynamic mechanical analysis (DMA) and rheological experiments show that increasing styrene content improves the mechanical properties of the triblocks co-PILs (Figures S2 and S3).

Density and Volume Fraction Estimation. The densities of the polyIL homopolymers, poly(1-[ω-methacryloyloxydecyl]-3-(n-butyl)-imidazolium X^-) (poly(1BDIMAX)), where X^- corresponds to

DOI: 10.1021/acs.macromol.8b02143
Macromolecules 2019, 52, 620−628

Table 2. Molecular Weights and Volume Fractions of Triblock Co-PolyILs, Poly(S-*b*-1BDIMAX-*b*-S), for Different Counteranions

M_n (kg/mol)	3−34−3			9−34−9			15−34−9		
counterions	Br	BF_4	NTf_2	Br	BF_4	NTf_2	Br	BF_4	NTf_2
φ_{PIL}	0.84	0.84	0.82	0.64	0.64	0.61	0.51	0.52	0.48

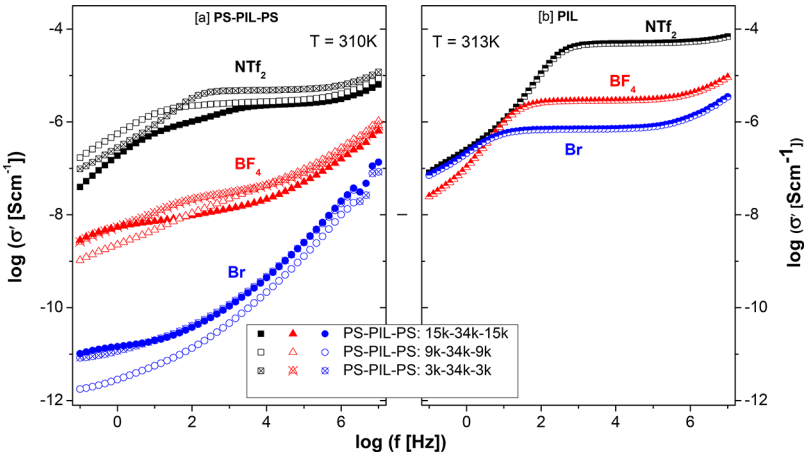

Figure 3. (a) Real part of complex conductivity $\sigma^* = \sigma' + i\sigma''$ as a function of frequency for triblock co-PILs with bromide, Br (circles), tetrafluoroborate, BF_4 (triangles), and bis(trifluoromethylsulfonyl)imide, NTf_2 (squares), anions at 310 K. Panel (b) shows corresponding data for the homo-PIL systems as indicated measured at 313 K.

bromide (Br^-), tetrafluoroborate (BF_4^-), and bis(trifluoromethylsulfonyl)imide (NTf_2^-), were estimated as

$$\frac{1}{\rho} = \frac{w_{NMA}}{\rho_{NMA}} + \frac{w_{IL}}{\rho_{IL}}$$

where w_i is the molecular weight fraction of the nonyl methacrylate (NMA) and ionic liquid (IL) moieties of the monomer and ρ_i is the density of the corresponding moiety. The densities of the IL components were calculated based on the ionic volumes of the IL constituents.[45] The densities of $bmim^+Br^-$, $bmim^+BF_4^-$, and $bmim^+NTf_2^-$ were calculated to be 1.43, 1.36, and 1.63 g cm^{-3}, respectively. The density of NMA is 0.97 g cm^{-3}. As an example, the density of the homopolyIL, poly(1BDIMANTf$_2$) is calculated as

$$\frac{1}{\rho} = \frac{0.3362}{0.97\ \text{g cm}^{-3}} + \frac{0.6638}{1.63\ \text{g cm}^{-3}}$$

$$\rho \approx 1.33\ \text{g cm}^{-3}$$

The density of poly(1BDIMABr) was determined to be 1.16 g cm^{-3}, and the density of poly(1BDIMABF_4) was calculated as 1.14 g cm^{-3}.

The volume fractions were calculated using

$$\varphi_{PIL} = \frac{M_{n_{PIL}}/\rho_{PIL}}{\left(\frac{M_{n_{PIL}}}{\rho_{PIL}}\right) + \left(\frac{M_{n_S}}{\rho_S}\right)}$$

where M_{n_i} is the number-average molecular weight of the corresponding block and ρ_i is the density of the block. The density of poly(styrene) (PS) is 1.05 g cm^{-3}. For the triblock copolyILs, the number-average molecular weight of the poly(styrene) blocks was taken to be the sum of the molecular weights of the two PS end blocks. The calculated volume fractions for each molecular weight and counteranion are given in Table 2.

RESULTS AND DISCUSSION

Broadband dielectric spectroscopy (BDS) is used to determine the real and imaginary part of the complex conductivity, $\sigma^* = \sigma' + i\sigma''$. Figure 3 presents the real part, σ', of the complex conductivity as a function of frequency for both the triblock co-PILs and the homo-PILs as measured at ∼37 °C. In disordered ionic materials, the ionic conductivity typically exhibits three key frequency regions in σ': frequency dependence in the high frequency regime, an intermediate frequency-independent dc ionic conductivity plateau, and interfacial/electrode polarization at low frequencies. This trend is well-approximated by the random barrier model (RBM), in which the charge transport in disordered systems is thought to proceed by hopping of the charge carriers in a random spatially varying landscape of potential energy barriers.[46,47] To contribute to dc ionic conductivity, σ_0, the charge carriers must overcome the highest energy barrier and participate in long-range ion diffusion. The rate at which this occurs is the characteristic ion diffusion rate, which marks the transition from frequency-dependent to frequency-independent σ'. At sufficiently long time scales the accumulation of charge carriers leads to electrode polarization, which decreases ionic conductivity at lower frequencies.

Because of interfacial polarization effects between charged and noncharged blocks in the ionic triblock copolymers, a well-defined plateau in σ' is absent in some of the compositions studied. An alternative analysis involving the dielectric loss modulus $M'' = \frac{\omega\varepsilon_0\sigma''}{(\sigma')^2 + (\sigma'')^2}$ (where ε_0 is the permittivity of free space and ω the radial frequency of the applied field) was therefore applied; here, the characteristic ion diffusion rate roughly corresponds to the peak frequency. The dc ionic conductivity, σ_0, is then extracted from the value of σ' at the time scale of the characteristic ion diffusion rate corresponding to the peak in M'' (Figure 4). Because the extraction of σ_0 is based on the determination of the ion diffusion rate, as a next step, we checked how values of the characteristic ion diffusion rates obtained from different approaches compare. Data for the sample PS−PIL−PS(3K−34K−3K)NTf_2 which has a better defined plateau than most of the other samples was used for this check. Ion diffusion rates were obtained from the peak in the derivative form of the dielectric loss ($\varepsilon''_{der}(\omega) = (-\pi/$

DOI: 10.1021/acs.macromol.8b02143
Macromolecules 2019, 52, 620−628

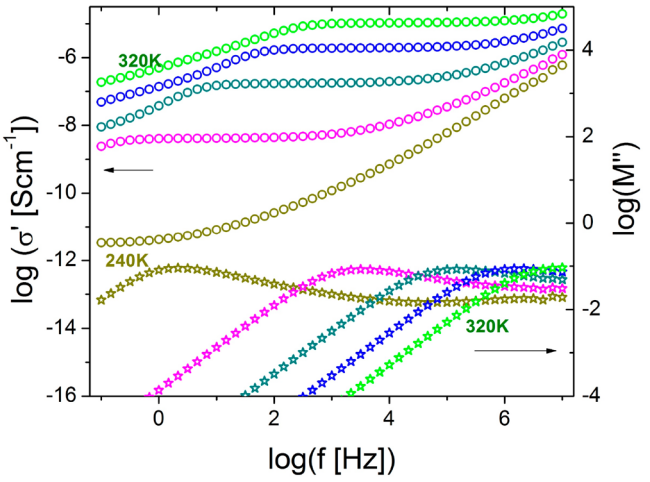

Figure 4. Real part σ' of the complex conductivity (circles) and the dielectric loss modulus M'' (stars) plotted as functions of frequency at temperatures between 240 and 320 K in steps of 20 K for the PS–PIL–PS(3K–34K–3K)NTf_2 sample.

2)$[\partial\varepsilon'(\omega)/\partial \ln \omega]$; see Figure 5a) and from a function combining the random barrier model and the empirical Havriliak–Negami equation (i.e.

$$\varepsilon^* = \frac{\sigma_0}{i\omega\varepsilon_0}\frac{i\omega\tau_e}{\ln(1+i\omega\tau_e)} + \mathcal{E}_\infty + \frac{\Delta\varepsilon}{[1+(i\omega\tau_{HN})^\alpha]^\gamma} + A(\omega)^n$$

where σ_0 is the dc ionic conductivity, $\mathcal{E}_\infty$ is the high-frequency limiting permittivity, $\Delta\varepsilon$ is the dielectric strength, τ_e and τ_{HN} are the relaxation times, and α and γ are the stretching parameters. The pre-exponential factor A and the exponent n of the power-law function account for the low-frequency dispersion due to interfacial polarization fitted to the real and imaginary parts of the complex permittivity. Figure 5b shows the values of the characteristic ion diffusion rates determined from the three approaches; while there is some disparity at higher temperatures, the values obtained via determination of the peak in M'' compare well with those obtained from the other approaches.

Figure 6 shows the temperature dependence of the dc ionic conductivity for all studied systems. We observe that the ionic conductivity values are higher in the homo-PILs than their corresponding triblock counterparts by about 1 order of magnitude for the NTf_2 species and up to 4 orders for Br and assign this to the reduced volume fraction (see Table 2) of the charge-carrying block in the latter systems. It is also clear that dc ionic conductivity is highest for the systems with NTf_2 anion, followed by BF_4 and then Br. This is consistent with the fact that T_g values increase in the same order. The influence of the choice of anion on dc ionic conductivity has been observed before in related systems[42,48−53] and ascribed to counterion size effects and Coulombic interactions: bulkier anions—as opposed to smaller ones (e.g., Br) which interact more strongly—plasticize the polymer matrices by inducing weaker electrostatic interactions, resulting in decreasing T_g (from 22 °C (Br) to −10 °C (BF_4) and −31 °C (NTf_2); see Table 1). It is important to note here that the anion size conductivity dependence holds for the homo-PILs as well as the triblock co-PILs, implying that the mechanism of ion transport is similar for both systems. This idea is lent credence by the fact that the temperature dependence of the characteristic relaxation rates for ion dynamics for both homo-PILs and triblock co-PILs coincide into a single curve when normalized by the corresponding temperatures, T_c, at which the dynamics have a common rate (see the inset of Figure 8).

At room temperature (vertical line, Figure 6), ionic conductivity is increased by 6 orders of magnitude through substituting the Br anion with NTf_2. While the size and charge distribution of the anion account for this change, such a tremendous increase via a simple ion exchange protocol has not been observed before for homo-PILs. To gain further

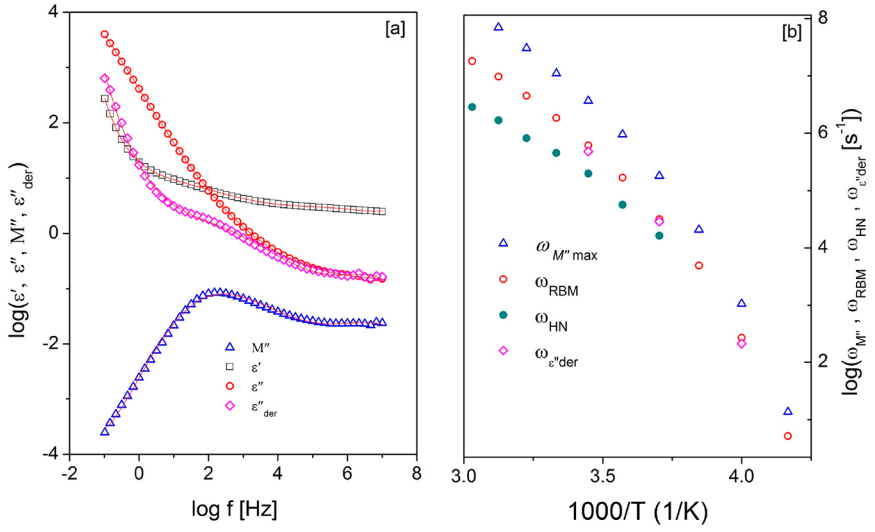

Figure 5. (a) Real (ε') and imaginary part (ε'') of the complex permittivity, the dielectric loss modulus (M''), and the derivative representation of the dielectric loss (ε''_{der}) plotted as functions of frequency as measured at 250 K for PS–PIL–PS(3K–34K–3K)NTf_2. Solid lines are fits to the data using the models discussed in the text. (b) Temperature dependence of the characteristic ion diffusion rates as obtained via four different approaches: from the maximal position of the dielectric loss modulus (triangles), from a function comprising the random barrier model and the Havriliak–Negami equation (open circles), and from HN fits to the derivative representation of the dielectric loss (diamonds). [For completeness, the closed circles represent the HN part of the RBN + HN function mentioned above; this accounts for the reorientation polarization arising from the motion of the ions.]

DOI: 10.1021/acs.macromol.8b02143
Macromolecules 2019, 52, 620−628

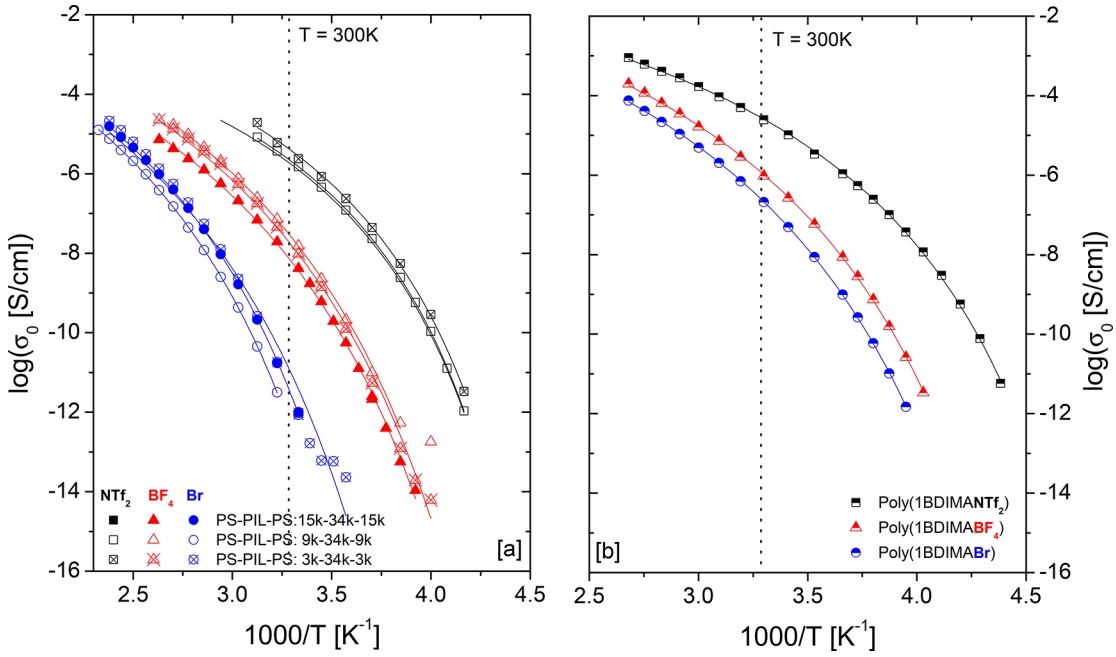

Figure 6. The dc ionic conductivity as a function of inverse temperature for (a) triblock co-PILs and corresponding (b) homo-PILs with bromide, Br (circles), tetrafluoroborate, BF_4 (triangles), and bis(trifluoromethylsulfonyl)imide, NTf_2 (squares), anions. The vertical dotted lines indicate room temperature (T = 300 K), while the solid lines are fits to the Vogel−Fulcher−Tammann equation. The fit parameters are presented in Table S1 of the Supporting Information.

insight into this, dc ionic conductivity is plotted as a function of T_g-normalized temperature (Figure 7). This representation

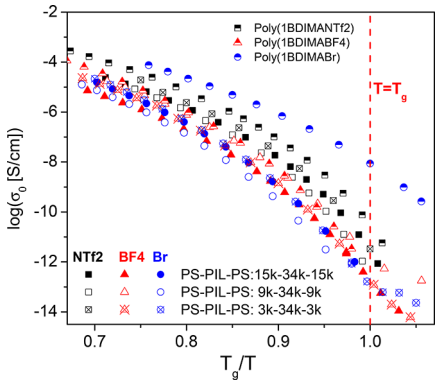

Figure 7. The dc ionic conductivity as a function of T_g-normalized temperature for all systems reported in this work. Half-filled symbols denote homo-PILs while the rest are triblock co-PILs, as indicated.

compares ionic conductivity in terms of the structural relaxation of the polymer matrix and so suppresses differences in properties such as T_g, and to some extent molecular weight, hence allowing a direct comparison of ion transport with respect to the structural relaxation. Typically, ionic conductivity in homo-PILs follows a Vogel−Fulcher−Tammann (VFT)-like temperature dependence above T_g where the motion of the ions is aided by structural dynamics of the polymer. Below T_g, the molecular motion of the polymer is frozen with respect to the experimental time scales, and ion transport exhibits Arrhenius-like temperature dependence. In this study, T_g-independent dc ionic conductivity does not show any significant decoupling of ion dynamics from the structural relaxation—as is characteristic for many homo-PILs, which typically exhibit σ_0 values of 10^{-6}−10^{-8} S/cm at T_g.[54] Instead, the T_g-independent values for the triblock co-PILs are comparable to those of low molecular weight ionic liquid systems with σ_0 in the range 10^{-12}−10^{-13} S/cm (at T_g).[55] We attribute this to the long flexible alkyl spacer separating the cationic groups from the structural relaxation of the polymer backbone, giving the imidazolium cation more degrees of freedom for its rotational and translational motion, similar to low molecular weight ionic liquid systems.[42] This qualitative picture also clarifies why ion exchange causes drastic changes in dc ionic conductivity.

In the triblock co-PILs presented here, the molecular weight of the noncharged polystyrene bock is varied from 6 to 30 kg/mol while that of the charged block is kept constant. This results in changes in the volume fraction of the charged block from 0.51 to 0.84 for Br and BF_4 systems and 0.48 to 0.82 for NTf_2 (see Table 2). It is likely that microphase morphology could be altered by these changes. Although this aspect is not explicitly investigated in this work (preliminary X-ray diffraction experiments show no obvious long-range morphological differences between the samples; Figure S4), we note that for any given counterion the length of the noncharged block has a negligible effect on dc ionic conductivity. This suggests that charge transport proceeds solely through the charged block, in effect providing a handle for enhancing mechanical properties without impeding ion transport.

To quantify the shift in the dc ionic conductivity of the triblock co-PILs with respect to the homo-PILs, a normalized conductivity can be determined to be $\sigma_N = \sigma_0/\sigma_c\varphi_c$, where σ_0 is the measured dc ionic conductivity of the triblock co-PIL, σ_c is the measured dc ionic conductivity of the conducting phase, and φ_c is the volume fraction of the conducting phase.[37,56,57] This equation would yield a value of unity for the case where the ionic conductivity of the triblock co-PIL matches that of the homo-PIL when weighted by the volume fraction of the conducting block. It is observed (see Figure 9) that values of

DOI: 10.1021/acs.macromol.8b02143
Macromolecules 2019, 52, 620−628

the normalized conductivity are significantly less than unity and fall dramatically with decreasing temperature. We hypothesize that the rigidity of the high-T_g polystyrene blocks imposes restriction on the motion of the conducting phase, causing the ionic conductivity to fall rapidly as the system is cooled. This effect of the styrene end blocks is rationalized by the decrease in the characteristic ion diffusion rates of the triblock co-PILs compared to their homo-PIL analogues (Figure 8). At room temperature, going from the homo-PILs to the triblock co-PILs, the diffusion rates fall by about 1 order of magnitude for the NTf_2, 2 orders for BF_4, and 5 orders for Br.

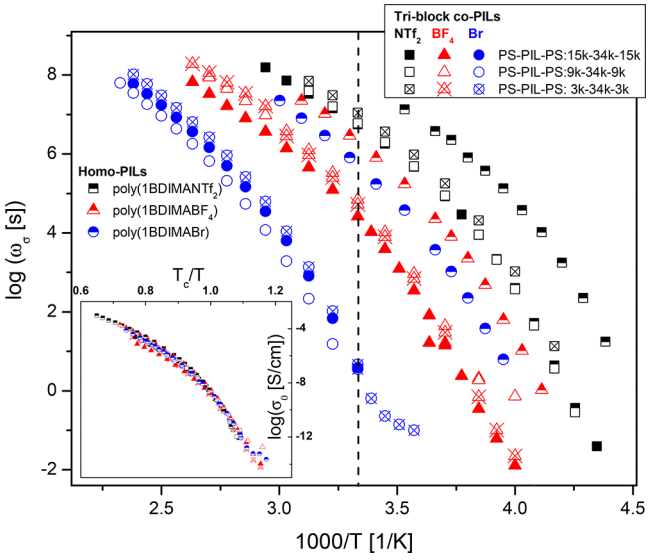

Figure 8. Temperature dependence of characteristic ion diffusion rates for the different samples of triblock co-PILs and their corresponding homo-PILs. The vertical dashed line marks room temperature. Inset: dc ionic conductivity plotted against T_c-normalized temperature, where T_c is the temperature at which the characteristic charge transport rate is 4 rad/s.

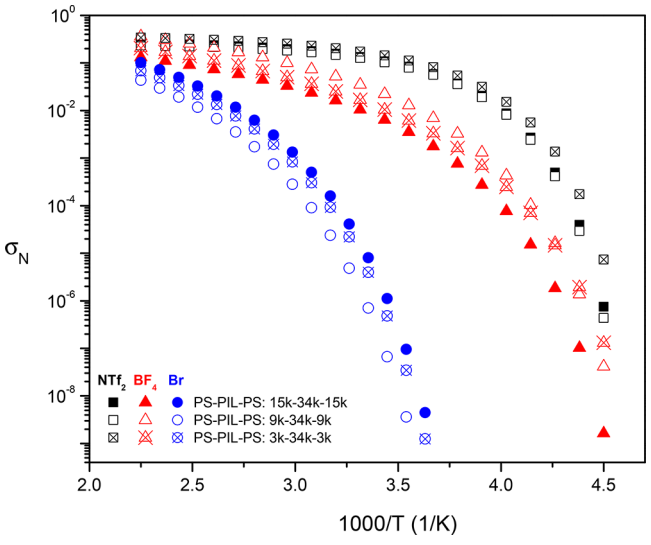

Figure 9. Normalized conductivity, σ_N, plotted as a function of inverse temperature for the triblock co-polyILs. The normalized conductivity is calculated as $\sigma_N = \sigma_0/\sigma_c\varphi_c$, where σ_0 is the measured dc ionic conductivity of the triblock co-polyIL, σ_c is the measured dc ionic conductivity of the conducting phase, and φ_c is the volume fraction of the conducting phase.

CONCLUSION

Novel ionic triblock copolymers were synthesized and investigated using differential scanning calorimetry (DSC) and broadband dielectric spectroscopy (BDS). By varying the molecular weight of noncharged polystyrene block and keeping that of the charged PIL block constant, the volume fraction of the latter was tuned in the range ~0.5 to ~0.8 for a series of samples with Br, BF_4, and NTF_2 anions. T_g-independent ionic conductivity is comparable to that of low molecular weight ILs rather than typical homo-PILs due to the placement of the cations relative to the polymer backbone: the long alkyl spacer between charged imidazolium moieties and polymer backbones offered extra mobility to the ion pairs, allowing an increase in ionic conductivity by over 6 orders of magnitude through facile counterion exchange. For the same counterions, ionic conductivity shows no dependence on the length of the polystyrene blocks, promising an unprecedented means to control polymer viscoelastic properties without altering ionic conductivity.

ASSOCIATED CONTENT

Supporting Information

The Supporting Information is available free of charge on the ACS Publications website at DOI: 10.1021/acs.macromol.8b02143.

^{1}H NMR, DMA, and SAXS data; VFT fit parameters (PDF)

AUTHOR INFORMATION

Corresponding Authors

*E-mail jsangoro@utk.edu.
*E-mail lokitzbs@ornl.gov.

ORCID

Emmanuel U. Mapesa: 0000-0002-2206-0990
Thomas Kinsey: 0000-0002-1107-4449
Yangyang Wang: 0000-0001-7042-9804
Timothy E. Long: 0000-0001-9515-5491
Bradley S. Lokitz: 0000-0002-1229-6078
Joshua R. Sangoro: 0000-0002-5483-9528

Author Contributions

E.U.M. and M.C. equally contributed to this work.

Notes

The authors declare no competing financial interest.

ACKNOWLEDGMENTS

This manuscript has been authored by UT-Battelle, LLC, under Contract DE-AC05-00OR22725 with the U.S. Department of Energy. E.U.M., M.A.H., and M.F.H. are grateful for financial support by the National Science Foundation, Division of Materials Research, Polymers Program, through DMR-1508394. J.S. gratefully acknowledges partial support from the U.S. Army Research Office under Contract W911NF-17-1-0052. This research was suported by Oak Ridge National Laboratory's (ORNL) Laboratory Directed Research and Development Program. A portion of this work was conducted at the Center for Nanophase Materials Sciences, which is a US Department of Energy Office of Science User Facility. This

DOI: 10.1021/acs.macromol.8b02143
Macromolecules 2019, 52, 620−628

work is also supported by the US National Science Foundation under Award DMR 1507764.

REFERENCES

(1) MacFarlane, D. R.; Tachikawa, N.; Forsyth, M.; Pringle, J. M.; Howlett, P. C.; Elliott, G. D.; Davis, J. H.; Watanabe, M.; Simon, P.; Angell, C. A. Energy applications of ionic liquids. *Energy Environ. Sci.* **2014**, *7* (1), 232−250.
(2) Hall, C. C.; Zhou, C.; Danielsen, S. P. O.; Lodge, T. P. Formation of Multicompartment Ion Gels by Stepwise Self-Assembly of a Thermoresponsive ABC Triblock Terpolymer in an Ionic Liquid. *Macromolecules* **2016**, *49* (6), 2298−2306.
(3) Moon, H. C.; Kim, C. H.; Lodge, T. P.; Frisbie, C. D. Multicolored, Low-Power, Flexible Electrochromic Devices Based on Ion Gels. *ACS Appl. Mater. Interfaces* **2016**, *8* (9), 6252−60.
(4) Lee, J. H.; Lee, A. S.; Hong, S. M.; Hwang, S. S.; Koo, C. M. Hybrid ionogels derived from polycationic polysilsesquioxanes for lithium ion batteries. *Polymer* **2017**, *117*, 160−166.
(5) Lodge, T. P. Materials science - A unique platform for materials design. *Science* **2008**, *321* (5885), 50−51.
(6) Lodge, T. P.; Ueki, T. Mechanically Tunable, Readily Processable Ion Gels by Self-Assembly of Block Copolymers in Ionic Liquids. *Acc. Chem. Res.* **2016**, *49* (10), 2107−2114.
(7) Moon, H. C.; Kim, C. H.; Lodge, T. P.; Frisbie, C. D. Multicolored, Low-Power, Flexible Electrochromic Devices Based on Ion Gels. *ACS Appl. Mater. Interfaces* **2016**, *8* (9), 6252−6260.
(8) Jo, G.; Ahn, H.; Park, M. J. Simple Route for Tuning the Morphology and Conductivity of Polymer Electrolytes: One End Functional Group is Enough. *ACS Macro Lett.* **2013**, *2* (11), 990−995.
(9) Cotanda, P.; Petzetakis, N.; Jiang, X.; Stone, G.; Balsara, N. P. Hydroxide-ion transport and stability of diblock copolymers with a polydiallyldimethyl ammonium hydroxide block. *J. Polym. Sci., Part A: Polym. Chem.* **2017**, *55* (13), 2243−2248.
(10) Jyothi, M. S.; Soontarapa, K.; Padaki, M.; Balakrishna, R. G.; Isloor, A. M. Favorable influence of mPIAM on PSf blend membranes for ion rejection. *J. Membr. Sci.* **2017**, *533*, 229−240.
(11) Gao, R. L.; Wang, D.; Heflin, J. R.; Long, T. E. Imidazolium sulfonate-containing pentablock copolymer-ionic liquid membranes for electroactive actuators. *J. Mater. Chem.* **2012**, *22* (27), 13473−13476.
(12) Jangu, C.; Wang, J.-H. H.; Wang, D.; Sharick, S.; Heflin, J. R.; Winey, K. I.; Colby, R. H.; Long, T. E. Well-Defined Imidazolium ABA Triblock Copolymers as Ionic-Liquid-Containing Electroactive Membranes. *Macromol. Chem. Phys.* **2014**, *215*, 1319−1331.
(13) Margaretta, E.; Fahs, G. B.; Inglefield, D. L.; Jangu, C.; Wang, D.; Heflin, J. R.; Moore, R. B.; Long, T. E. Imidazolium-Containing ABA Triblock Copolymers as Electroactive Devices. *ACS Appl. Mater. Interfaces* **2016**, *8* (2), 1280−1288.
(14) Bara, J. E.; Lessmann, S.; Gabriel, C. J.; Hatakeyama, E. S.; Noble, R. D.; Gin, D. L. Synthesis and Performance of Polymerizable Room-Temperature Ionic Liquids as Gas Separation Membranes. *Ind. Eng. Chem. Res.* **2007**, *46* (16), 5397−5404.
(15) Bara, J. E.; Hatakeyama, E. S.; Gin, D. L.; Noble, R. D. Improving CO_2 permeability in polymerized room-temperature ionic liquid gas separation membranes through the formation of a solid composite with a room-temperature ionic liquid. *Polym. Adv. Technol.* **2008**, *19* (10), 1415−1420.
(16) Moghadam, F.; Kamio, E.; Yoshioka, T.; Matsuyama, H. New approach for the fabrication of double-network ion-gel membranes with high CO_2/N-2 separation performance based on facilitated transport. *J. Membr. Sci.* **2017**, *530*, 166−175.
(17) Yuan, J.; Mecerreyes, D.; Antonietti, M. Poly(ionic liquid)s: An update. *Prog. Polym. Sci.* **2013**, *38* (7), 1009−1036.
(18) Yuan, J.; Antonietti, M. Poly(ionic liquid)s: Polymers expanding classical property profiles. *Polymer* **2011**, *52* (7), 1469−1482.
(19) Hemp, S. T.; Zhang, M. Q.; Allen, M. H.; Cheng, S. J.; Moore, R. B.; Long, T. E. Comparing Ammonium and Phosphonium Polymerized Ionic Liquids: Thermal Analysis, Conductivity, and Morphology. *Macromol. Chem. Phys.* **2013**, *214* (18), 2099−2107.
(20) Wang, S.-W.; Liu, W.; Colby, R. H. Counterion Dynamics in Polyurethane-Carboxylate Ionomers with Ionic Liquid Counterions. *Chem. Mater.* **2011**, *23* (7), 1862−1873.
(21) Jourdain, A.; Serghei, A.; Drockenmuller, E. Enhanced Ionic Conductivity of a 1,2,3-Triazolium-Based Poly(siloxane ionic liquid) Homopolymer. *ACS Macro Lett.* **2016**, *5* (11), 1283−1286.
(22) Hemp, S. T.; Zhang, M.; Allen, M. H.; Cheng, S.; Moore, R. B.; Long, T. E. Comparing Ammonium and Phosphonium Polymerized Ionic Liquids: Thermal Analysis, Conductivity, and Morphology. *Macromol. Chem. Phys.* **2013**, *214* (18), 2099−2107.
(23) Snyder, J. F.; Carter, R. H.; Wetzel, E. D. Electrochemical and Mechanical Behavior in Mechanically Robust Solid Polymer Electrolytes for Use in Multifunctional Structural Batteries. *Chem. Mater.* **2007**, *19*, 3793−3801.
(24) Sangoro, J. R.; Iacob, C.; Agapov, A. L.; Wang, Y.; Berdzinski, S.; Rexhausen, H.; Strehmel, V.; Friedrich, C.; Sokolov, A. P.; Kremer, F. Decoupling of ionic conductivity from structural dynamics in polymerized ionic liquids. *Soft Matter* **2014**, *10* (20), 3536−40.
(25) Mogurampelly, S.; Keith, J. R.; Ganesan, V. Mechanisms Underlying Ion Transport in Polymerized Ionic Liquids. *J. Am. Chem. Soc.* **2017**, *139* (28), 9511−9514.
(26) Fan, F.; Wang, Y.; Hong, T.; Heres, M. F.; Saito, T.; Sokolov, A. P. Ion Conduction in Polymerized Ionic Liquids with Different Pendant Groups. *Macromolecules* **2015**, *48* (13), 4461−4470.
(27) Choi, U. H.; Ye, Y.; Salas de la Cruz, D.; Liu, W.; Winey, K. I.; Elabd, Y. A.; Runt, J.; Colby, R. H. Dielectric and Viscoelastic Responses of Imidazolium-Based Ionomers with Different Counterions and Side Chain Lengths. *Macromolecules* **2014**, *47* (2), 777−790.
(28) Wojnarowska, Z.; Feng, H.; Fu, Y.; Cheng, S.; Carroll, B.; Kumar, R.; Novikov, V. N.; Kisliuk, A. M.; Saito, T.; Kang, N.-G.; Mays, J. W.; Sokolov, A. P.; Bocharova, V. Effect of Chain Rigidity on the Decoupling of Ion Motion from Segmental Relaxation in Polymerized Ionic Liquids: Ambient and Elevated Pressure Studies. *Macromolecules* **2017**, *50* (17), 6710−6721.
(29) Fan, F.; Wang, W.; Holt, A. P.; Feng, H.; Uhrig, D.; Lu, X.; Hong, T.; Wang, Y.; Kang, N.-G.; Mays, J.; Sokolov, A. P. Effect of Molecular Weight on the Ion Transport Mechanism in Polymerized Ionic Liquids. *Macromolecules* **2016**, *49* (12), 4557−4570.
(30) Wojnarowska, Z.; Knapik, J.; Jacquemin, J.; Berdzinski, S.; Strehmel, V.; Sangoro, J. R.; Paluch, M. Effect of Pressure on Decoupling of Ionic Conductivity from Segmental Dynamics in Polymerized Ionic Liquids. *Macromolecules* **2015**, *48* (23), 8660−8666.
(31) Allen, M. H.; Hemp, S. T.; Zhang, M.; Zhang, M.; Smith, A. E.; Moore, R. B.; Long, T. E. Synthesis and characterization of 4-vinylimidazole ABA triblock copolymers utilizing a difunctional RAFT chain transfer agent. *Polym. Chem.* **2013**, *4* (7), 2333.
(32) Cotanda, P.; Petzetakis, N.; Jiang, X.; Stone, G.; Balsara, N. P. Hydroxide-ion transport and stability of diblock copolymers with a polydiallyldimethyl ammonium hydroxide block. *J. Polym. Sci., Part A: Polym. Chem.* **2017**, *55* (13), 2243−2248.
(33) Margaretta, E.; Fahs, G. B.; Inglefield, D. L., Jr.; Jangu, C.; Wang, D.; Heflin, J. R.; Moore, R. B.; Long, T. E. Imidazolium-Containing ABA Triblock Copolymers as Electroactive Devices. *ACS Appl. Mater. Interfaces* **2016**, *8* (2), 1280−8.
(34) Harris, M. A.; Heres, M. F.; Coote, J.; Wenda, A.; Strehmel, V.; Stein, G. E.; Sangoro, J. Ion Transport and Interfacial Dynamics in Disordered Block Copolymers of Ammonium-Based Polymerized Ionic Liquids. *Macromolecules* **2018**, *51* (9), 3477−3486.
(35) Ye, Y.; Choi, J.-H.; Winey, K. I.; Elabd, Y. A. Polymerized Ionic Liquid Block and Random Copolymers: Effect of Weak Microphase Separation on Ion Transport. *Macromolecules* **2012**, *45* (17), 7027−7035.
(36) Weber, R. L.; Ye, Y.; Schmitt, A. L.; Banik, S. M.; Elabd, Y. A.; Mahanthappa, M. K. Effect of Nanoscale Morphology on the Conductivity of Polymerized Ionic Liquid Block Copolymers. *Macromolecules* **2011**, *44* (14), 5727−5735.

DOI: 10.1021/acs.macromol.8b02143
Macromolecules 2019, 52, 620−628

(37) Choi, J.-H.; Ye, Y.; Elabd, Y. A.; Winey, K. I. Network Structure and Strong Microphase Separation for High Ion Conductivity in Polymerized Ionic Liquid Block Copolymers. *Macromolecules* **2013**, *46* (13), 5290−5300.
(38) Ye, Y.; Sharick, S.; Davis, E. M.; Winey, K. I.; Elabd, Y. A. High Hydroxide Conductivity in Polymerized Ionic Liquid Block Copolymers. *ACS Macro Lett.* **2013**, *2* (7), 575−580.
(39) Virgili, J. M.; Hexemer, A.; Pople, J. A.; Balsara, N. P.; Segalman, R. A. Phase Behavior of Polystyrene-*block*-poly(2-vinylpyridine) Copolymers in a Selective Ionic Liquid Solvent. *Macromolecules* **2009**, *42* (13), 4604−4613.
(40) Hoarfrost, M. L.; Segalman, R. A. Ionic Conductivity of Nanostructured Block Copolymer/Ionic Liquid Membranes. *Macromolecules* **2011**, *44* (13), 5281−5288.
(41) Schneider, Y.; Modestino, M. A.; McCulloch, B. L.; Hoarfrost, M. L.; Hess, R. W.; Segalman, R. A. Ionic Conduction in Nanostructured Membranes Based on Polymerized Protic Ionic Liquids. *Macromolecules* **2013**, *46* (4), 1543−1548.
(42) Chen, M.; Dugger, J. W.; Li, X.; Wang, Y.; Kumar, R.; Meek, K. M.; Uhrig, D. W.; Browning, J. F.; Madsen, L. A.; Long, T. E.; Lokitz, B. S. Polymerized ionic liquids: Effects of counter-anions on ion conduction and polymerization kinetics. *J. Polym. Sci., Part A: Polym. Chem.* **2018**, *56* (13), 1346−1357.
(43) Allen, M. H.; Hemp, S. T.; Zhang, M. S.; Zhang, M. Q.; Smith, A. E.; Moore, R. B.; Long, T. E. Synthesis and characterization of 4-vinylimidazole ABA triblock copolymers utilizing a difunctional RAFT chain transfer agent. *Polym. Chem.* **2013**, *4* (7), 2333−2341.
(44) Anastasaki, A.; Nikolaou, V.; McCaul, N. W.; Simula, A.; Godfrey, J.; Waldron, C.; Wilson, P.; Kempe, K.; Haddleton, D. M. Photoinduced Synthesis of alpha,omega-Telechelic Sequence-Controlled Multiblock Copolymers. *Macromolecules* **2015**, *48* (5), 1404−1411.
(45) Marcus, Y. Ionic and molar volumes of room temperature ionic liquids. *J. Mol. Liq.* **2015**, *209*, 289−293.
(46) Dyre, J. C. The random free-energy barrier model for ac conduction in disordered solids. *J. Appl. Phys.* **1988**, *64* (5), 2456−2468.
(47) Schrøder, T. B.; Dyre, J. C. Computer simulations of the random barrier model. *Phys. Chem. Chem. Phys.* **2002**, *4* (14), 3173−3178.
(48) Godeau, G.; Navailles, L.; Nallet, F.; Lin, X.; McIntosh, T. J.; Grinstaff, M. W. From Brittle to Pliant Viscoelastic Materials with Solid State Linear Polyphosphonium - Carboxylate Assemblies. *Macromolecules* **2012**, *45* (5), 2509−2513.
(49) Abdulahad, A. I.; Jangu, C.; Hemp, S. T.; Long, T. E. Influence of Counterion on Thermal, Viscoelastic, and Ion Conductive Properties of Phosphonium Ionenes. *Macromol. Symp.* **2014**, *342* (1), 56−66.
(50) Tudryn, G. J.; Liu, W.; Wang, S.-W.; Colby, R. H. Counterion Dynamics in Polyester−Sulfonate Ionomers with Ionic Liquid Counterions. *Macromolecules* **2011**, *44* (9), 3572−3582.
(51) Tao, R.; Tamas, G.; Xue, L.; Simon, S. L.; Quitevis, E. L. Thermophysical Properties of Imidazolium-Based Ionic Liquids: The Effect of Aliphatic versus Aromatic Functionality. *J. Chem. Eng. Data* **2014**, *59* (9), 2717−2724.
(52) Chen, S.; Funtan, A.; Gao, F.; Cui, B.; Meister, A.; Parkin, S. S. P.; Binder, W. H. Synthesis and Morphology of Semifluorinated Polymeric Ionic Liquids. *Macromolecules* **2018**, *51*, 8620.
(53) Chen, S.; Frenzel, F.; Cui, B.; Gao, F.; Campanella, A.; Funtan, A.; Kremer, F.; Parkin, S. S. P.; Binder, W. H. Gating effects of conductive polymeric ionic liquids. *J. Mater. Chem. C* **2018**, *6* (30), 8242−8250.
(54) Iacob, C.; Matsumoto, A.; Brennan, M.; Liu, H.; Paddison, S. J.; Urakawa, O.; Inoue, T.; Sangoro, J.; Runt, J. Polymerized Ionic Liquids: Correlation of Ionic Conductivity with Nanoscale Morphology and Counterion Volume. *ACS Macro Lett.* **2017**, *6* (9), 941−946.
(55) Sangoro, J. R. Charge transport and dipolar relaxations in an alkali metal oligoether carboxylate ionic liquid. *Colloid Polym. Sci.* **2014**, *292* (8), 1933−1938.
(56) Wanakule, N. S.; Panday, A.; Mullin, S. A.; Gann, E.; Hexemer, A.; Balsara, N. P. Ionic Conductivity of Block Copolymer Electrolytes in the Vicinity of Order−Disorder and Order−Order Transitions. *Macromolecules* **2009**, *42* (15), 5642−5651.
(57) Yuan, R.; Teran, A. A.; Gurevitch, I.; Mullin, S. A.; Wanakule, N. S.; Balsara, N. P. Ionic Conductivity of Low Molecular Weight Block Copolymer Electrolytes. *Macromolecules* **2013**, *46* (3), 914−921.

DOI: 10.1021/acs.macromol.8b02143
Macromolecules 2019, 52, 620−628